Dalton
www.rsc.org/dalton

Bis(*tert*-butylamido)- and bis(arylamido)cyclodiphosph(III)azane complexes of Ti, V, Zr and Hf: ligand substituent effects and coordination number

Daniel F. Moser,[a] Luke Grocholl,[a] Lothar Stahl*[a] and Richard J. Staples[b]

[a] *Department of Chemistry, University of North Dakota, Grand Forks, ND 58202-9024, USA. E-mail: lstahl@chem.und.edu*

[b] *Department of Chemistry and Chemical Biology, Harvard University, Cambridge, MA 02138, USA*

Received 8th November 2002, Accepted 11th February 2003
First published as an Advance Article on the web 26th February 2003

Syntheses and structures of $[\{(Bu^tNP)_2(Bu^tN)_2\}MCl_2]$, M = Zr, Hf, $[\{(Bu^tNP)_2(ArN)_2\}TiCl_2]$, Ar = Ph, *m*-Tol, *p*-Tol, and of $[\{(Bu^tNP)_2(PhN)_2\}VCl\cdot THF]$, are reported. In the solid-state these compounds are *seco*-heterocubic metal complexes featuring one η^3-coordinated bis(amido)cyclodiphosphazane ligand. When $ZrCl_4$ and $HfCl_4$ are treated with $\{(Bu^tNP)_2(PhNLi\cdot THF)_2\}$, however, the diligand complexes $[\{(Bu^tNP)_2(PhN)_2\}_2M]$, M = Zr, Hf are isolated.

Introduction

Amido-complexes of early transition metals are electronically and often coordinatively unsaturated species,[1] that are useful in the activation of small molecules,[2] polymerization catalysis[3] and as precursors for metal nitrides.[4] Because of this versatility much effort has gone into tuning the reactivity of such compounds with purpose-specific bulky monodentate[5] or multidentate[6] ligands. Our interest in the synthesis of nitrogen-donor complexes of early transition metals was spurred by reports that certain bis(amido)metal dichloride complexes of Group 4 metals are highly-active, living homogeneous polyolefin catalysts.[7] We introduced bis(*tert*-butylamido)cyclodiphosph(III)azanes as possible variants of chelating diamides,[8] because the U-shaped structure of these ligands is conducive to creating monomeric pseudo-tetrahedral complexes. Some time ago we communicated syntheses and structures of $[\{(Bu^tNP)_2(Bu^tN)_2\}MCl_2]$, M = Zr (**1**), Hf (**2**)—the first transition metal complexes of these ligands.[9] Here we report full synthetic and structural details of these compounds and the extension of this chemistry to related metals and ligands.

The utility of homogeneous polyolefin catalysts is determined by both metal and ligand. Thus, titanocenes and vanadocenes with identical ligands often have very different properties,[10] vanadocenes typically being less active but producing polymers of higher molecular weights. Similarly large effects are observed upon subtle ligand modifications for catalysts with identical metal centers. To further explore the structural chemistry of bis(amido)cyclodiphosph(III)azanes and their complexes, we expanded our investigations to vanadium and to ligands with the sterically smaller anilino and toluidino substituents. Below we report the full synthetic and structural details of bis(*tert*-butylamido)- and bis(arylamido)-cyclodiphosph(III)azanes and their mono- and diligand complexes of Group 4 and 5 metals.

Results and discussion

The reaction of MCl_4 (M = Zr, Hf) with $\{(Bu^tNP)_2(Bu^tNLi\cdot THF)_2\}$ (Scheme 1) is highly solvent dependent, affording $[\{(Bu^tNP)_2(Bu^tN)_2\}MCl_2]$, M = Zr (**1**), Hf (**2**) reproducibly from hot toluene, but leading to intractable mixtures when done in THF. Both Group 4 metal complexes were isolated as moderately moisture-sensitive, light-yellow or cream-colored solids, respectively.

The compounds crystallize isostructurally as molecular solids without unusual intermolecular contacts. Listings of the

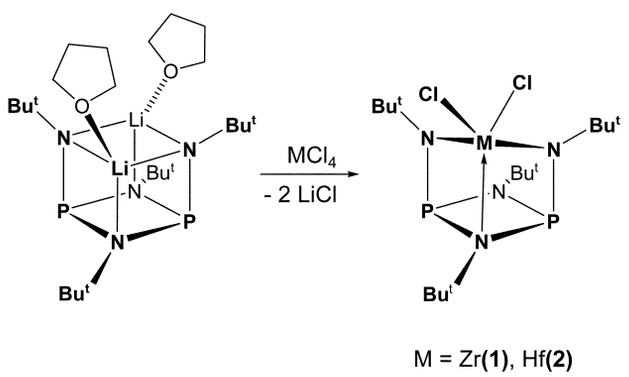

Scheme 1

data collection and selected bond parameters of these complexes are given in Tables 1 and 2, respectively. The ORTEP drawing of **1** (Fig. 1) depicts the pseudo-trigonal bipyramidal coordination of the zirconium atom, while that of **2** (Fig. 2) emphasizes the deviation of the metal atom from a central position above the heterocycle. Because both complexes are isostructural, only the hafnium complex will be discussed in detail. Although the coordination geometry of the hafnium atom is close to trigonal-bipyramidal in the solid state, the long

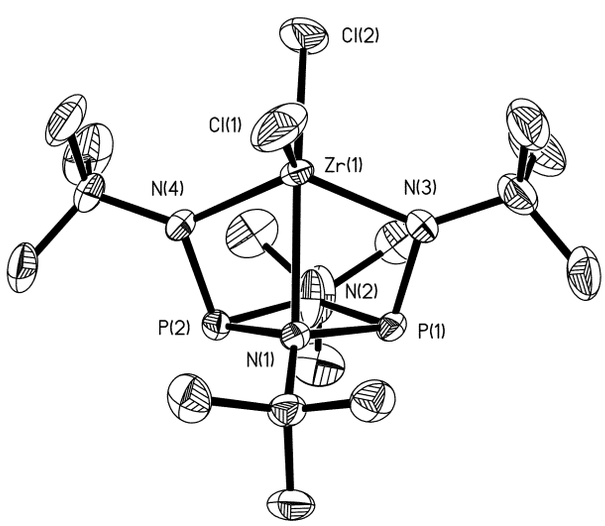

Fig. 1 Thermal-ellipsoid (35%) plot and partial numbering scheme of **1**. Hydrogen atoms have been omitted for clarity.

DOI: 10.1039/b211009a

Table 1 Crystal and refinement data for **1**, **2**, **4a**, **5a**, **6**, **7**·$C_6H_5CH_3$, **8a** and **9**

Compound	**1**	**2**	**4a**	**5a**	**6**	**7**·$C_6H_5CH_3$	**8a**	**9**
Formula	$C_{16}H_{36}Cl_2N_4P_2Zr$	$C_{16}H_{36}HfCl_2N_4P_2$	$C_{20}H_{30}N_4P_2$	$C_{28}H_{44}N_4Li_2O_2P_2$	$C_{40}H_{56}N_8P_2Zr$	$C_{47}H_{64}HfN_8P_4$	$C_{20}H_{28}Cl_2N_4P_2Ti$	$C_{26}H_{36}ClN_4OP_2V$
Formula weight	508.55	595.82	388.42	544.49	864.03	1043.43	505.20	544.90
Crystal system	orthorhombic	orthorhombic	monoclinic	monoclinic	orthorhombic	triclinic	monoclinic	monoclinic
Space group	$P2_12_12_1$ (no. 19)	$P2_12_12_1$ (no. 19)	$C2/c$ (no. 15)	$P2_1/c$ (no. 14)	*Pbcn* (no. 60)	$P\bar{1}$ (no. 2)	Cc (no. 9)	$P2_1/c$ (no. 14)
a/Å	9.921(2)	9.937(3)	16.7769(5)	17.701(5)	21.7990(5)	11.994(3)	9.2541(3)	10.4689(1)
b/Å	15.129(3)	15.132(4)	5.8729(2)	11.549(2)	9.7180(2)	13.134(4)	15.4971(6)	12.8799(2)
c/Å	16.331(4)	16.414(5)	22.4726(6)	17.547(4)	20.4069(4)	16.365(5)	16.7405(6)	20.9860(1)
α/°	90	90	90	90	90	90.765(10)	90	90
β/°	90	90	102.090(1)	118.772(8)	90	101.60(3)	94.248(10)	102.520(1)
γ/°	90	90	90	90	90	99.39(2)	90	90
U/Å^3	2451.2(8)	2468(1)	2165.1(1)	3144(1)	4323.1(2)	2488(7)	2394.2(2)	2762.43(5)
Z	4	4	4	4	4	2	4	4
μ/mm^{-1}	0.805	4.580	0.212	0.168	0.441	2.264	0.729	0.595
Reflections collected	9072	6141	5239	12959	18997	10087	7805	17903
Independent reflections (R_{int})	4921 (0.0248)	3078 (0.0221)	1848 (0.0415)	5416 (0.0361)	4688 (0.0407)	8716 (0.0326)	3819 (0.0238)	5822 (0.0335)
$R(F)$ ($I > 2\sigma I$)[a]	0.0412	0.0472	0.0449	0.0609	0.0384	0.0413	0.0240	0.0355
$wR_2(F^2)$[b]	0.1017	0.1138	0.1357	0.1436	0.0880	0.1110	0.0654	0.0952

[a] $R = \Sigma||F_o| - |F_c||/\Sigma|F_o|$. [b] $wR_2 = \{[\Sigma\, w(F_o^2 - F_c^2)^2]/[\Sigma w(F_o^2)^2]\}^{1/2}$; $w = 1/[\sigma^2(F_o)^2 + (xP)^2 + yP]$ where $P = (F_o^2 + 2F_c^2)/3$.

Table 2 Selected bond lengths (Å) and angles (°) for **1** and **2**

	1	**2**
M–Cl(avg.)	2.377(2)	2.368(5)
M–N(amido, avg.)	2.064(3)	2.067(9)
M–N(imido)	2.398(3)	2.394(9)
P(1,2)–N(1,avg.)	1.785(3)	1.787(10)
P(1,2)–N(2,avg.)	1.736(3)	1.743(10)
P(1,2)–N(3,4)	1.682(3)	1.648(9)
Cl(1)–M–Cl(2)	104.51(8)	103.7(2)
Cl(1)–M–N(1)	100.82(9)	100.8(2)
Cl(2)–M–N(1)	154.66(10)	155.5(3)
N(3)–M–N(4)	124.62(13)	124.8(4)

((2.394(9) Å) and weak N–Hf donor bond makes it more appropriate to describe the coordination number of the metal as 4 + 1. The hafnium–chloride and hafnium–amide bonds have average lengths of 2.368(5) and 2.067(9) Å, respectively and are thus similar to the corresponding bonds in a 1,2-benzenediamidozirconium dichloride(THF) dimer, which feature Zr–N and terminal Zr–Cl bonds of 2.049(5) and 2.403(2) Å length, respectively.[11] Because of the planarity of the amido groups in **1** and **2**, it may be assumed that there is at least some π-bonding between ligand and metal, making these ligands possible 8 electron donors and raising the electron-count at the metal to 14 electrons. While the donor bond from the basal nitrogen atom (N1) creates a C_s-symmetric ground-state, the equivalence of the ring-*tert*-butyl substituents in the NMR spectra supports a time-averaged C_{2v} symmetry in solution.

Fig. 2 Thermal-ellipsoid (35%) plot and partial numbering scheme of **2**. Hydrogen atoms have been omitted for clarity.

The regio- and stereoselectivities of homogeneous catalysts depend largely on ligand effects. C_s- and C_2-symmetric metallocenes of identical metals and cocatalysts, for example, produce syndiotactic and isotactic polypropylene, respectively. In order to build symmetry and steric effects into cyclodiphosphazane ligands, we began using 2,4-diarylamino-substituted heterocycles,[12] because aromatic amines with a variety of substituents are commercially available. Although a 1,3-diphenyl-2,4-dianilino-substituted cyclodiphosph(III)azane, namely, *cis*-{Ph(H)NP(μ-NPh)$_2$PN(H)Ph} is available in a one-step synthesis,[13] its low solubility makes it an unsuitable ligand.

We had previously described the synthesis of *cis*-{Ph(H)-NP(μ-NBu^t)$_2$PN(H)Ph} (**4a**) from *cis*-{ClP(μ-NBu^t)$_2$PCl} [14] (**3**) and lithium anilide.[12] Here we report the syntheses of the *m*- and *p*-tolylamino analogues, which are outlined in Scheme 2, as well as the solid-state structure of **4a**. This compound, whose data collection and bond parameters are listed in Tables 1 and 2, crystallizes in the form of colorless rods in the monoclinic crystal system. The isolated molecules are stacked along the

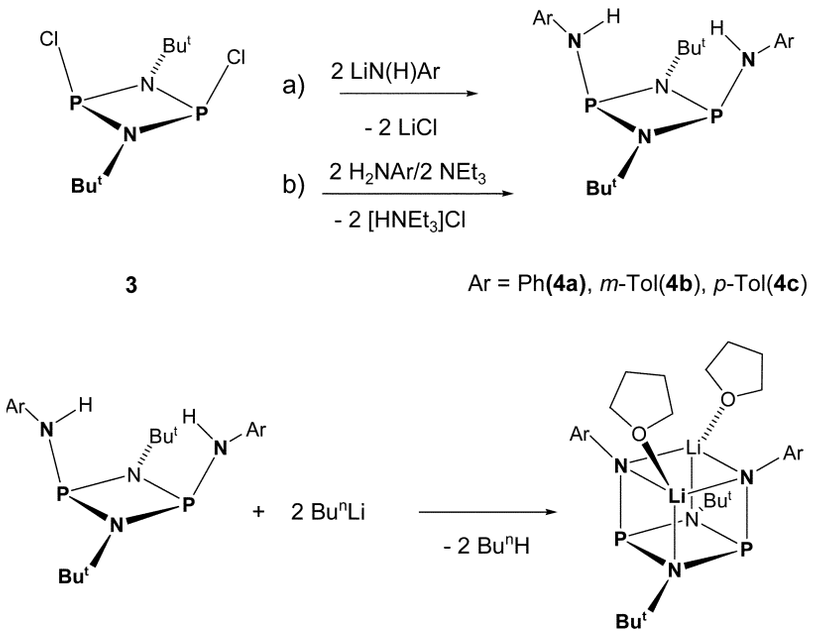

Scheme 2

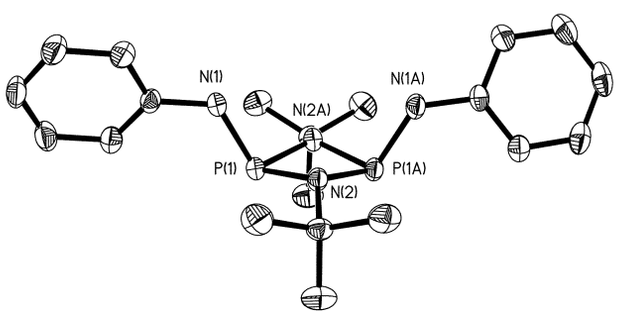

Fig. 3 Thermal-ellipsoid (35%) plot and partial numbering scheme of **4a**. Hydrogen atoms have been omitted for clarity.

twofold axes of the space group *C*2/*c*, giving them, analogous to *cis*-{Bu^t(H)NP(μ-NBu^t)$_2$PN(H)Bu^t},[8] crystallographic two-fold-rotation symmetry.

The thermal-ellipsoid plot of **4a** (Fig. 3) emphasizes the greater span, but comparatively lesser steric bulk of the phenyl groups, which are in an *exo*-orientation with respect to the heterocycle. This highly-puckered central ring has equidistant P–N bonds (avg. 1.731(2) Å) and bears almost perpendicularly disposed anilino groups, whose P–N bonds (1.689(2) Å) are significantly shorter than those of the heterocycle.

Bis(arylamino)cyclodiphosph(III)azanes, like **4a**, **4b** and **4c**, are readily converted to their dilithio salts by treatment with *n*-butyllithium, as shown in Scheme 2, affording thermally stable, but air-sensitive, crystalline solids. An X-ray analysis of **5a**, an ORTEP drawing of which is shown in Fig. 4, revealed the common heterocubic structure that had also been observed for the *tert*-butyl analogue.[8] Crystal data and selected bond parameters of **5a** are collected in Tables 1 and 3.

The central portion of the molecule is a rhombically-distorted cube of P, N and Li atoms, which enclose angles ranging from 75 to 100°. While the bond lengths and angles are unremarkable and similar to those in the *tert*-butyl analogue,[8] the Li–O bonds of **5a** are significantly (*ca.* 0.1 Å) shorter than those in the *tert*-butyl analogue, and this may reflect either the compactness of the phenyl substituents or their lesser electron-donating ability.

Treatment of MCl_4, M = Zr, Hf, with {(Bu^{t}NP)$_2$(PhNLi·THF)$_2$} (Scheme 3), under the same conditions as those used for the syntheses of **1** and **2**, yielded the off-white, crystalline solids **6** and **7**. The NMR spectra of these species showed equally symmetrical peak patterns as those of **1** and **2**, but the negative

Table 3 Selected bond lengths (Å) and angles (°) for **4a** and **5a**

4a [a]			
P(1)–N(1)	1.689(2)	N(1)–P(1)–N(2)	104.84(11)
P(1)–N(2)	1.730(2)	N(1)–P(1)–N(2A)	104.83 (11)
P(1)–N(2A)	1.723(2)	N(2)–P(1)–N(2A)	80.96(11)
		P(1)–N(2)–P(1A)	96.86(11)
5a			
P–NBu^t(avg.)	1.763(3)	NBu^t–P–NBu^t(avg.)	83.04(13)
P–NPh(avg.)	1.677(3)	NPh–P–NBu^t(avg.)	98.07(12)
Li–NPh(avg.)	2.076(6)	Li–NPh–Li(avg.)	75.1(2)
Li–NBu^t(avg.)	2.094(6)	NPh–Li–NPh(avg.)	100.4(3)
Li–O(avg.)	1.870(6)	P–NBu^t–P(avg.)	96.93(13)

[a] Symmetry transformations used to generate equivalent atoms for **4a**: $-x + 2, y, -z + 1/2$.

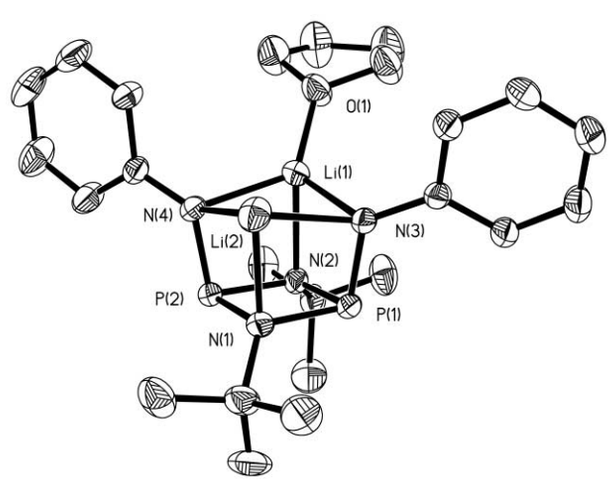

Fig. 4 Thermal-ellipsoid (35%) plot and partial numbering scheme of **5a**. The THF molecule coordinated to Li(2) and hydrogen atoms have been omitted for clarity.

Table 4 Selected bond lengths (Å) and angles (°) for **6** and **7**·$C_6H_5CH_3$

	6	**7**·$C_6H_5CH_3$
M–N(am., avg.)	2.157(2)	2.125(4)
M–N(im., avg.)	2.393(2)	2.396(4)
P–N(endoc., avg.)	1.750(2)	1.758(4)
P–N(exoc., avg.)	1.701(2)	1.700(4)
N–M–N(am., avg.)	108.04(8)	107.86(14)
N(am.)–M–N(im., avg.)	134.37(9)	140.11(12)

chloride-tests were consistent only with diligand complexes of the formula [{($Bu^tNP)_2(PhN)_2$}$_2$M], M = Zr (**6**), Hf (**7**).

Crystals, suitable for X-ray diffraction studies, were obtained for both compounds, although those of the hafnium analogue were isolated only as a toluene solvate, namely [{($Bu^tNP)_2$-$(PhN)_2$}$_2$Hf·$C_6H_5CH_3$]. Crystal and refinement parameters for **6** and **7**·$C_6H_5CH_3$ are listed in Table 1 and selected bond lengths and angles are given in Table 4. The ORTEP drawing of **6** (Fig. 5) emphasizes the crystallographic twofold-rotation symmetry of the compound, while that of **7**·$C_6H_5CH_3$ (Fig. 6) depicts the structural relationship of these diligand complexes to their monoligand counterparts **1** and **2**.

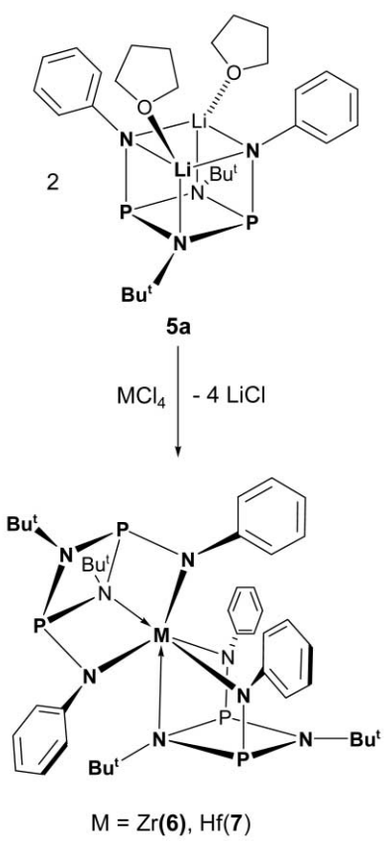

Scheme 3

Complexes **6** and **7** are the first bis(amido)cyclodiphosph(III)-azane derivatives in which the central metal atom is sandwiched between two η^3-coordinated bis(amido)cyclodiphosph(III)-azanes. The diligand coordination is a strong indication that the anilido-substituted ligand is sterically less encumbered than the *tert*-butyl-substituted analogue, because for the latter ligand disubstitution has not yet been observed. As was the case for the monoligand complexes **1** and **2**, the coordination environments about the Group 4 metals cannot be described in terms of conventional geometries, being neither octahedral nor trigonal prismatic. The four metal–amido bonds are almost tetrahedrally-disposed about the metal atom, with N–M–N angles ranging from 92.44(14) to 140.25(14)°. Their zirconium–amide

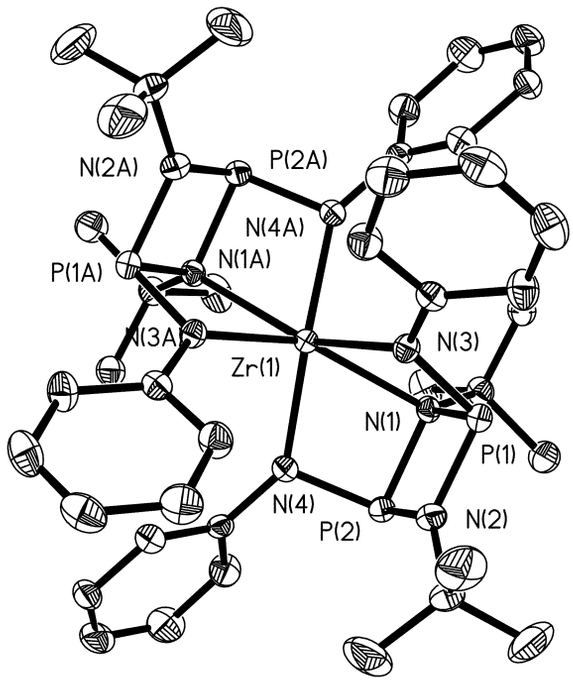

Fig. 5 Thermal-ellipsoid (35%) plot and partial numbering scheme of **6**, viewed along the crystallographic twofold-rotation axis. Hydrogen atoms have been omitted for clarity.

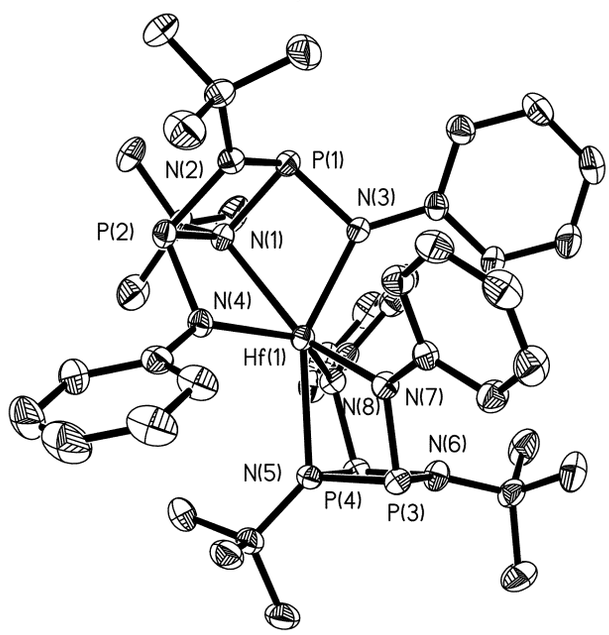

Fig. 6 Thermal-ellipsoid (35%) plot and partial numbering scheme of **7**·$C_6H_5CH_3$. Hydrogen atoms and toluene moiety have been omitted for clarity.

bonds (avg. 2.157(2) Å) are *ca.* 0.1 Å longer than those in **1** and **2**, but they are somewhat shorter than the Zr–N bonds (2.197(6) Å) in a related pseudo-octahedral bis(aminotroponiminato)zirconium dichloride complex.[15] Two long (2.393(2) Å) N–Zr donor bonds complete the coordination sphere of **6**.

The appearance of all chemically-equivalent *tert*-butyl groups as one signal in the low-temperature ^{1}H and ^{13}C NMR spectra of **6** and **7** shows that the diligand complexes exhibit similar fluxionalities as **1** and **2** and with similarly low activation energies. The disubstitution in **6** and **7** can be rationalized by the low solubility of MCl_4, even in hot toluene, resulting in the ligation of the much more soluble {($Bu^tNP)_2(PhN)_2MCl_2$} by the second equivalent of ligand, in preference to MCl_4. All attempts at obtaining monoligand complexes in solvents in which the MCl_4 starting materials are more soluble failed, just

Table 5 Selected bond lengths (Å) and angles (°) for **8a** and **9**

	8a	**9**
M–Cl	2.2460(6)	2.2918(7)
M–O		2.1028(14)
M–N(amido, avg.)	1.929(2)	1.9429(7)
M–N(imido)	2.267(2)	2.1588(7)
P–N(endocyc., avg.)	1.744(2)	1.7952(8)
P–N(exocyc., avg.)	1.727(2)	1.7088(7)
Cl(1)–M–O(or Cl2)	100.63(3)	92.38(4)
Cl(1)–M–N(1)	158.76(5)	106.35(5)
O(or Cl2)–M–N(1)	100.59(5)	161.19(6)
N(3)–M–N(4)	114.27(8)	109.49(7)

as it had in the case of **1** and **2**. Because their metal atoms are completely sterically shielded, **6** and **7** are obviously unsuitable candidates for catalytic applications.

The steric crowding in **6** and **7** caused us to consider the much smaller titanium (r_{cov} = 1.34 Å) as a candidate for monoligand derivatives of the more compact aryl-substituted ligands **4a**, **4b** and **4c**. Treatment of titanium tetrachloride with the corresponding dilithiobis(amido)cyclodiphosphazanes (**5a**–**5c**), however, was accompanied by considerable reduction of the titanium ion and led to a mixture of products. The target compounds were cleanly synthesized by treating $TiCl_4 \cdot (THF)_2$ with **4a**, **4b** or **4c** in the presence of triethylamine (Scheme 4); these reactions afforded diamagnetic orange–red to purple crystalline solids in good yields. Diligation of titanium was not only avoided, but it was, in fact, impossible to substitute titanium with two ligands even when **4a**, **4b** or **4c** were present in large excess. The solution NMR data of **8a**, **8b** and **8c** are similar to those of the zirconium and hafnium complexes exhibiting equivalent aryl and *tert*-butyl groups and are thus consistent with symmetrical solution-structures.

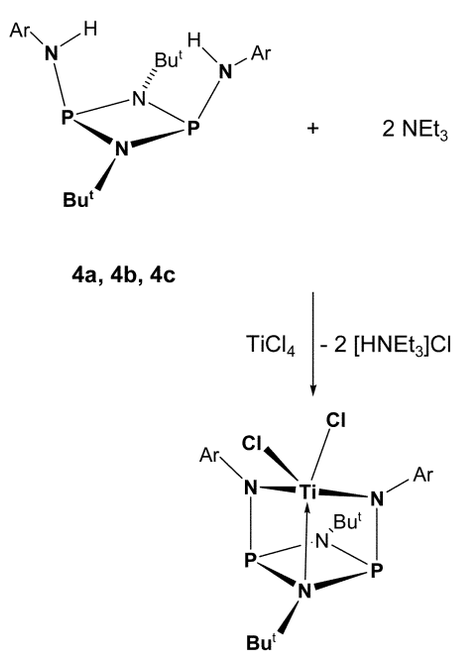

Scheme 4

Crystal and refinement parameters for **8a** are listed in Table 1 and selected bond parameters of **8a** are given in Table 5. The ORTEP view of **8a** in Fig. 7 emphasizes the high symmetry of this *seco*-heterocubic complex and the lesser steric crowding about the titanium atom. As expected, most of the bond parameters are identical to those of the *tert*-butyl analogue,[16]

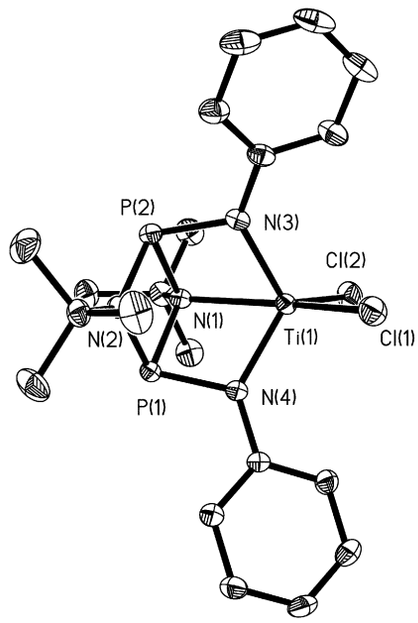

Fig. 7 Thermal-ellipsoid (35%) plot and partial numbering scheme of **8a**. Hydrogen atoms have been omitted for clarity.

but **8a** has a noticeably wider coordination gap, and this may have implications for metal-centered reactions of these complexes. The titanium–amide (1.929(2) Å) and titanium–chloride (2.2460(6) Å) bonds are identical to those in the *tert*-butyl analogue[16] and in related diamido-titanium dichlorides, but the Ti–amide bonds are slightly longer. For comparison, the Ti–N and Ti–Cl bonds in [{1,2-(NSiPr$^i_3$)benzene}$TiCl_2$] are 1.880(4) and 2.234(2) Å long,[17] respectively, while the corresponding bonds in [{1,3-(N-2,6-Pr^{i}Ph)propyl}$TiCl_2$] are 1.847(5) and 2.248(2) Å long.[18] The N–Ti donor bond (2.267(2) Å) of **8a** is of comparable length to those in the zirconium and hafnium species, when the smaller radius of titanium (1.34 *vs.* 1.45 Å) is taken into account.

The title complexes thus share a number of structural similarities with metal derivatives of the diamide {1,2-(NSiPr$^i_3$)-benzene}$^{2-}$,[17] which afforded diligand complexes for the larger zirconium, namely, [{1,2-(NSiPr$^i_3$)benzene}$_2$Zr] (**A**, shown in Chart 1), but monoligand species for titanium, namely, [{1,2-(NSiPr$^i_3$)benzene}$TiCl_2$] (**B**). Moreover these 1,2-bis(amido)-benzene complexes also feature weak, secondary interactions with the aromatic linker.

Although the bis(amido)cyclodiphosphazane ligands of the title compounds display η^3-coordination in the solid state, the NMR data on the diamagnetic derivatives are consistent only with molecules of higher symmetries. In solution, therefore, the metal atoms cannot be significantly associated with the basal imido atom even at temperatures as low as −80 °C. It appears that, as the result of the basket-shaped structure of the bis-(amido)cyclodiphosphazanes, the metal atoms are forced to be close to the ring-nitrogen atoms, without significant bond formation.

This behavior is in contrast to that of the related bis-(amido)amine zirconium complexes of the type $[N_2NX]ZrMe_2$ (**C**) reported by Schrock *et al.*, which exhibit bis(amido)amino coordination.[19] In these latter compounds the Zr–N(amido) (2.095(6) Å) and Zr–N(amino) (2.380(6) Å) bonds are almost identical in length to those in **1** and **2**, but with the notable exception that the donor bond formed by the sp^3-hybridized amine atom is static.

To date no bis(amido)cyclodiphosph(III)azane compound for a transition metal from Groups 5 through 9 has been reported. It was therefore of interest to see if a bis(anilido)cyclodiphosphazane complex of vanadium chloride would be accessible. Treatment of $VCl_3 \cdot (THF)_3$ with **5a** in toluene (Scheme 5)

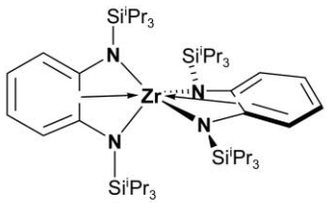

A

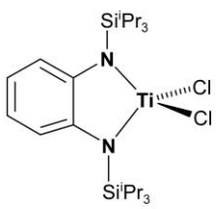

B

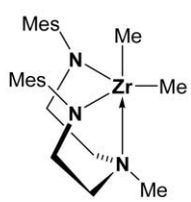

C

Chart 1

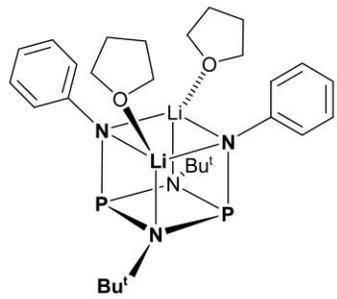

5a

$VCl_3(THF)_3$ | - 2 LiCl

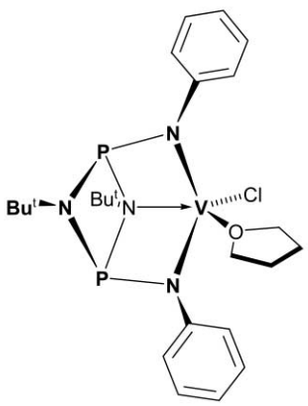

9

Scheme 5

produced an orange–brown solution from which dark-red crystals of **9** deposited on cooling. In solution this compound exhibited an effective magnetic moment of 2.59 Bohr magnetons, consistent with a vanadium(III) ion, having two unpaired electrons.

Lack of NMR-spectroscopic information necessitated an X-ray structural analysis, the data-collection parameters of which are listed in Table 1. Selected bond parameters of this compound are compared with those of the related **8a** in Table 5. The thermal-ellipsoid plot of **9**, which is shown in Fig. 8, emphasizes the *seco*-heterocubic nature of this complex and its structural relationship to **1**, **2** and **8a**. Thus, the vanadium atom has pseudo trigonal-bipyramidal geometry, being η^3-coordinated by the chelating diamide, one chloride ligand and one molecule of tetrahydrofuran. The metal–amide and metal–chloride bond lengths of **9** are similar to those of **8a**, despite the smaller covalent radius (1.22 Å) of vanadium. Solely the N–V donor bond of **9** (2.1588(7) Å) is significantly shorter than that of **8a** (2.267(2) Å). This dative interaction has lengthened the P–N bonds of the ring nitrogen (N1) atom from 1.735(2) Å in the pristine ligand **4a** to 1.7952(8) Å in the vanadium complex. The V–Cl (2.2918(7) Å), V–N(2, 3) (avg. 1.9429(7) Å) and V–O (2.1028(14) Å) bonds may be compared to those of azaatranevanadium(III) and azaatranevanadium(IV) complexes. Thus, for example, [{$N(CH_2CH_2NSiMe_3)_3$}VCl] (**D**, shown in Chart 2) features vanadium–amide, vanadium–amino and vanadium–chloride bonds of 1.880(6), 2.238(6) and 2.278(2) Å, respectively.[20] In the corresponding vanadium(III) species [{$N(CH_2CH_2NSiMe_3)_3$}V] (**E**) the amido–vanadium bonds are almost identical (avg. 1.930(6) Å) to those in **9**, but the lone donor bond is notably shorter (2.08 (6) Å), a feature which the authors ascribed to the absence of a second axial substituent.[21]

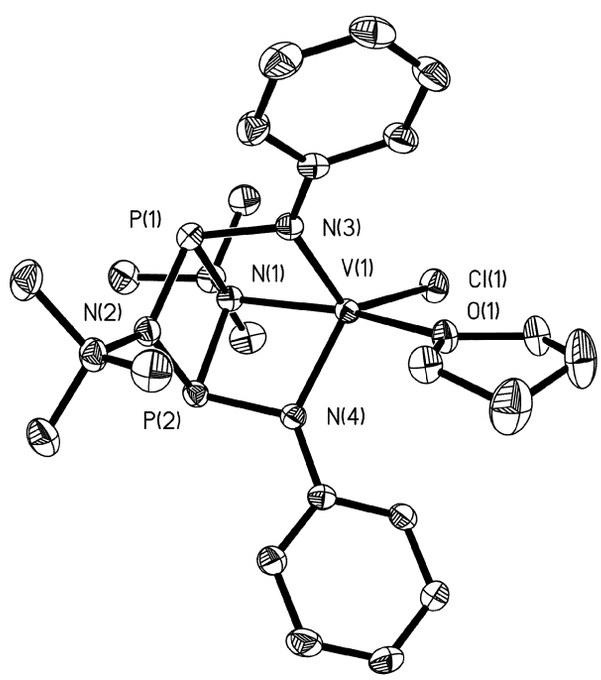

Fig. 8 Thermal-ellipsoid (35%) plot and partial numbering scheme of **9**. Hydrogen atoms have been omitted for clarity.

When compounds **1** and **2** were tested in polymerization studies, as outlined in the experimental section, no polymer was produced. Unexpectedly, however, **8a** did produce polyethylene, although its activity was approximately one order of magnitude lower than that of the precatalyst Cp_2ZrCl_2 under identical conditions. The phosphine odor emanating from the pressure vessel indicated that these reactions are accompanied by

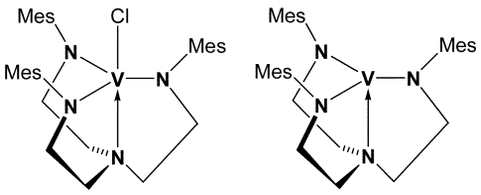

D E

Chart 2

considerable ligand degradation, likely brought on by the Lewis-acidic cocatalyst.[22] This makes it difficult to predict the true nature of the active species in the reaction mixture of **8a**, and we therefore hesitate to draw conclusion based on the structural differences of **1**, **2** and **8a**.

Both their instability and the ensuing odor compromise the use of the title complexes in polyolefin catalysis. Their electron deficiencies and low coordination numbers (**6** and **7** are exceptions), however, should render these complexes of interest for applications outside the realm of polymerization reactions. The instability of the title compounds may be advantageous for uses as molecular precursors of solid-state materials. For example, the ease of ring-opening of cyclodiphosph(III)azanes, perhaps in combination with labile $SiMe_3$ nitrogen substituents or ammonolysis, may lead to metal nitrides (M_xN_y) or metal nitride–phosphate compounds, *i.e.*, $M_xP_yN_z$.[23] Attempts of obtaining the former species from **1** were recently reported by Roesky *et al.*[24]

Conclusion

Bis(*tert*-butylamido)cyclodiphosph(III)azanes react with titanium, zirconium and hafnium tetrachlorides to form η^3-coordinated monoligand dichloro complexes, having trigonal-bipyramidally coordinated metal centers. The less bulky bis(arylamido)cyclodiphosph(III)azanes form similar monoligand complexes only with the 3d transition metals titanium and vanadium, while the larger zirconium and hafnium atoms form homoleptic complexes in which the Group 4 metal is coordinated by two ligand moieties. Only the bis(anilido)-cyclodiphosphazanetitanium dichloride compound polymerized ethylene in the presence of MAO, while the zirconium and hafnium analogues with bis(*tert*-butyl)cyclodiphosphazane ligands were inactive.

Experimental

All operations were performed under an atmosphere of argon or pre-purified nitrogen on conventional Schlenk lines or in a glove box. The hydrocarbon or ethereal solvents were pre-dried over molecular sieves or CaH_2 and distilled under a nitrogen atmosphere from sodium or potassium benzophenone ketyl immediately before use. The tetrachlorides of zirconium and hafnium were purchased from Aldrich and Aesar, respectively, and were used as received. Methylalumoxane (MAO) was purchased from Aldrich as a 10% wt. toluene solution. *Cis*-{Bu^t(H)NP(μ-NBu^t)$_2$PN(H)Bu^t},[8] *cis*-{Ph(H)NP(μ-NBu^t)$_2$PN(H)Ph},[12] *cis*-{(Bu^{t}NP)$_2$(Bu^{t}NLi·THF)$_2$},[8] and *cis*-{(Bu^{t}NP)$_2$(PhNLi·THF)$_2$}[12] were prepared by published procedures.

Mass spectra were recorded on a Finnigan MAT 95 in the chemical ionization mode, using methane as the reacting gas. NMR spectra were recorded on Varian VXR-300 and Bruker Avance-500 spectrometers. ^{1}H, ^{13}C and ^{31}P NMR spectra are referenced relative to C_6D_5H (7.15 ppm) C_6H_6 (128.0 ppm) and $P(OEt)_3$ (+ 137.0), respectively. Melting points were recorded on a Mel-Temp melting point apparatus; they are uncorrected. E & R Microanalytical Services, Parsippany, NJ, and Robertson Microlit Laboratories, Inc., Madison, NJ, performed the elemental analyses.

Syntheses

[{(Bu^{t}NP)$_2$(Bu^{t}N)$_2$}ZrCl$_2$] (1). Samples of *cis*-{(Bu^{t}NP)$_2$(Bu^{t}NLi·THF)$_2$}, (1.23 g, 2.43 mmol) and zirconium tetrachloride (0.594 g, 2.56 mmol) were combined in toluene (30 mL). The ensuing suspension was stirred at 80 °C for 1 d, cooled to 0 °C for 3 h, and then filtered through a medium-porosity frit. The light-yellow solution was concentrated to 10 mL *in vacuo* and then stored at −12 °C for 3 d. This produced light-yellow, columnar crystals (0.948 g, 1.86 mmol). Yield: 72.7%. Mp 215 °C. Found: C, 37.55; H, 6.89; N, 10.87. $C_{16}H_{36}Cl_2N_4P_2Zr$ requires C, 37.79; H, 7.13; N, 11.02%. δ_H (C_6D_6) 1.410 (18 H, s, Bu^t), 1.267 (18 H, s, Bu^t); δ_C (C_6D_6) 59.7 (d, J = 16 Hz), 55.26 (t, J = 11 Hz), 33.7 (d, J = 11 Hz), 30.1 (t, J = 6 Hz); δ_P (C_6D_6) 101.67; *m*/*z* (CI, methane) 509.78 $[M + H]^+$.

[{(Bu^{t}NP)$_2$(Bu^{t}N)$_2$Hf}Cl$_2$] (2). In a manner identical to that used for the synthesis of **1**, *cis*-{(Bu^{t}NP)$_2$(Bu^{t}NLi·THF)$_2$}, (1.26 g, 2.50 mmol) and hafnium tetrachloride (0.863 g, 2.69 mmol) were allowed to react in hot (80 °C) toluene (35 mL) for 2 d. The reaction produced cream-colored, bar-shaped crystals (1.20 g, 1.94 mmol) in a 72.1% yield. Mp 198 °C. Found: C, 32.34; H, 6.05; N, 9.20. $C_{16}H_{36}Cl_2N_4P_2Hf$ requires C, 32.25; H, 6.09; N, 9.40%. δ_H (C_6D_6) 1.398 (18 H, s, Bu^t), 1.270 (18 H, s, Bu^t); δ_C (C_6D_6) 58.4 (d, J = 16 Hz), 55.0 (t, J = 11 Hz), 33.8 (d, J = 9.0 Hz), 29.8 (t, J = 6.0 Hz); δ_P (C_6D_6) 99.85. *m*/*z* (CI, methane) 597.1 $[M + H]^+$.

***cis*-{ClP(μ-NBu^t)$_2$PCl} (3).** This is a modified version of a previously-published procedure.[14] A 2000 mL three-necked flask, equipped with addition funnel, magnetic stirbar and two inlets was charged with PCl_3 (27.5 g, 200 mmol), toluene (50 mL) and triethylamine (30.4 g, 300 mmol). To this cooled (−78 °C) solution was added *via* dropping funnel *tert*-butylamine (21.9 g, 300 mmol) dissolved in toluene (150 mL). The mixture was allowed to warm to RT, refluxed (3.5 h), stirred at RT (12 h) and then filtered. Toluene and excess amines were removed by ambient-pressure and vacuum distillations until a light-yellow oil remained. This solidified within 24 h to an off-white crystalline mass. Yield: 25.8 g (94%). Mp 42–46 °C. δ_H (C_6D_6) 1.17 (18 H, s, Bu^t); δ_C (C_6D_6) 54.3 (s), 30.2 (*s*); δ_P (C_6D_6) 205.8 (s).

***cis*-{*m*-Tol(H)NP(μ-NBu^t)$_2$PN(H)*m*-Tol} (4b).** In a cooled (0 °C) 250 mL two-neck flask, *m*-toluidine (1.34 g, 12.6 mmol), dissolved in THF (15 mL), was treated with n-butyllithium (5.03 mL, 12.6 mmol). The solution was allowed to warm to RT and then treated dropwise with a solution of **3** (1.73 g, 6.30 mmol), dissolved in toluene (12 mL). The ensuing yellow–orange reaction mixture was stirred at RT for 12 h. All volatile components were then removed *in vacuo*, and the solid residue was extracted with hexanes (20 mL). The extract was filtered through a medium-porosity frit, and the filtrate was concentrated until crystals formed. Upon refrigeration (−21 °C) colorless, rectangular crystals (1.96 g, 75.0%) separated from the solution. Mp 106–109 °C. Found: C, 63.66; H, 8.55; N, 13.69. $C_{22}H_{34}N_4P_2$ requires C, 63.45; H, 8.23; N, 13.45%. δ_H (C_6D_6) 7.09 (2 H, t, J_{HH} = 7.6 Hz), 6.97 (2 H, s), 6.93 (2 H, d, J_{HH} = 8.2 Hz), 6.68 (2 H, d, J_{HH} = 7.3 Hz), 4.77 (2 H, s, NH), 2.15 (6 H, s, Me), 1.31 (18 H, s, NBu^t); δ_C (C_6D_6) 143.5 (s), 139.0 (s), 129.3 (s), 122.1 (s), 119.4 (s), 119.4 (br s), 51.7 (t, J_{PC} = 13.6 Hz), 31.1 (t, J_{PC} = 6.3 Hz), 21.6 (s); δ_P (C_6D_6) 99.6 (s).

***cis*-{*p*-Tol(H)NP(μ-NBu^t)$_2$PN(H)*p*-Tol} (4c).** In a 200 mL two-necked flask, *p*-toluidine (0.771 g, 7.20 mmol) and triethylamine (1.00 mL, 7.20 mmol) were dissolved in 10 mL of

toluene. When this mixture was treated with a toluene solution (10 mL) of **3** (0.990 g, 3.60 mmol) a white precipitate formed. The reaction mixture was kept at 35 °C for 12 h, filtered through a medium-porosity frit and concentrated until crystals formed. The flask was stored in a freezer for 1 d to afford 1.10 g (73.0%) of colorless needles. Mp 162–164 °C. Found: C, 63.27; H, 8.52; N, 13.08. $C_{22}H_{34}N_4P_2$ requires C, 63.45; H, 8.23; N, 13.45%. δ_H (C_6D_6) 7.03 (4 H, d, J_{HH} = 8.4 Hz), 6.97 (4 H, d, J_{HH} = 8.4 Hz), 4.69 (2 H, s, NH), 2.12 (6 H, s, Me), 1.31 (18 H, s, NBu^t); δ_C (C_6D_6) 141.3 (s), 130.3 (s), 129.7 (s), 119.7 (br s), 52.0 (t, J_{PC} = 13.6 Hz), 31.5 (t, J_{PC} = 6.4 Hz), 21.1 (s); δ_P (C_6D_6) 100.4 (s).

{(Bu^{t}NP)$_2$(*m*-TolNLi·THF)$_2$} (5b). A 100 mL two-necked flask, equipped with inlet, stirbar and funnel was charged with **4b** (0.534 g, 1.28 mmol) and THF (15 mL). The flask was immersed in an ice bath and the solution was treated dropwise with n-butyllithium (1.10 mL, 2.75 mmol). The solution was refluxed (12 h) and then concentrated until crystals formed. After the flask had been stored in a freezer (−12 °C), colorless, block-shaped crystals (0.606 g, 82.8%) deposited. Mp 159–162 °C. Found: C, 62.77; H, 8.70; N, 9.59. $C_{30}H_{48}N_4Li_2O_2P_2$ requires C, 62.93; H, 8.45; N, 9.79%. δ_H (C_6D_6) 7.25 (4 H, t, J_{HH} = 7.6 Hz), 7.04 (2 H, d, J_{HH} = 8.0 Hz), 6.62 (2 H, d, J_{HH} = 7.2 Hz), 3.42 (8 H, m, THF), 2.34 (6 H, s, Me), 1.45 (18 H, s), 1.19 (8 H, m, THF); δ_C (C_6D_6) 156. 0 (d, J_{PC} = 24.3 Hz), 138.2 (s), 129.2 (s), 119.9 (d, J_{PC} = 24.3 Hz), 117.1 (d, J_{PC} = 19.8 Hz), 116.2 (s), 68.3 (s, THF), 52.3 (t, J_{PC} = 15.5 Hz), 30.1 (t, J_{PC} = 7.3 Hz), 25.4 (s), 22.1 (s, THF); δ_P (C_6D_6) 162.6 (s).

[{(Bu^{t}NP)$_2$(PhN)$_2$}$_2$Zr] (6). In a 100 mL two-necked flask, equipped with stirbar and inlet, $ZrCl_4$ (0.447 g, 1.92 mmol) and **5a** (1.04 g, 1.92 mmol) were dissolved in 25 mL of toluene, resulting in a bright-yellow suspension. The reaction mixture was stirred at 75 °C for 1 d, then cooled to 0 °C and filtered through a medium-porosity frit. The bright-yellow filtrate was concentrated *in vacuo* and kept at −12 °C for 3 d to afford 0.581 g (70.7%) of product. Mp 250 °C (dec.). Found: C, 55.60; H, 6.73; N, 12.85. $C_{40}H_{56}N_8P_4Zr$ requires C, 55.60; H, 6.53; N, 12.97%. δ_H (C_6D_6) 7.40 (4 H, d, J_{HH} = 7.8 Hz), 6.99 (4 H, t, J_{HH} = 7.7 Hz), 6.72 (2 H, t, J_{HH} = 6.8 Hz), 1.22 (18 H, s, Bu^t); δ_C (C_6D_6) 129.4 (d, J_{PC} = 17.6 Hz), 129.0 (s), 123.4 (d, J_{PC} = 14.5 Hz), 122.1 (s), 54.4 (t, J_{PC} = 11.3 Hz), 29.4 (t, J_{PC} = 7.7 Hz); δ_P (C_6D_6) 143.1 (s).

[{(Bu^{t}NP)$_2$(PhN)$_2$}$_2$Hf] (7). In a manner identical to that used for the synthesis of **6**, $HfCl_4$ (0.890 g, 2.78 mmol) and **5a** (3.03 g, 5.56 mmol) were combined and heated. The bright-yellow filtrate was concentrated *in vacuo* and kept at −12 °C for 12 h to afford 1.71 g (65.0%) of pale-yellow crystals. Mp 238–240 °C. Found: C, 50.30; H, 6.09; N, 11.58. $C_{40}H_{56}N_8P_4Hf$ requires C, 50.50; H, 5.93; N, 11.78%. δ_H (C_6D_6) 7.41 (4 H, d, J_{HH} = 7.8 Hz, arom. H), 6.99 (4 H, t, J_{HH} = 7.7 Hz, arom. H), 6.71 (2 H, t, J_{HH} = 6.9 Hz, arom. H), 1.22 (18 H, s, Bu^t); δ_C (C_6D_6) 129.4 (d, J_{PC} = 17.8 Hz), 129.0 (s), 123.7 (d, J_{PC} = 15.1 Hz), 122.1 (s), 54.4 (t, J_{PC} = 11.4 Hz), 29.4 (t, J_{PC} = 7.7 Hz); δ_P (C_6D_6) 146.1 (s).

[{(Bu^{t}NP)$_2$(PhN)$_2$}TiCl$_2$] (8a). In a 100 mL two-necked flask, triethylamine (0.430 mL, 3.08 mmol), 1.5 mL of a titanium tetrachloride stock solution and **4a** of were combined. After the flask had been stored at −21 °C for 24 h, 0.408 g (52.4%) of dark-red crystals were recovered. This and subsequent fractions yielded a total of 0.599 g (77.0%) of product. Mp 198–200 °C. Found: C, 47.75; H, 5.68; N, 10.98. $C_{20}H_{28}Cl_2N_4P_2Ti$ requires C, 47.55; H, 5.59; N, 11.09%. δ_H (C_6D_6) 7.45 (4 H, d, J_{HH} = 7.9 Hz), 7.11 (4 H, t, J_{HH} = 7.7 Hz), 6.85 (2 H, t, J_{HH} = 7.6 Hz), 1.11 (18 H, s, NBu^t). δ_C (C_6D_6) 153.4 (m), 129.1 (s), 125.2 (s), 121.3 (m), 54.7 (t, J_{PC} = 8.7 Hz), 28.1 (t, J_{PC} = 6.9 Hz). δ_P (C_6D_6) 127.6 (s).

[{(Bu^{t}NP)$_2$(*m*-TolN)$_2$}TiCl$_2$] (8b). The compound was prepared by combining 0.370 mL (2.67 mmol) of triethylamine, 1.30 mL (1.30 mmol) of a 1.0 M solution of $TiCl_4$ and 0.557 g (1.34 mmol) of **4b** in a manner identical to that used for the synthesis of **8a**. Overall yield: 0.501g (70.0%). Mp 139–141 °C. Found: C, 49.34; H, 6.22; N, 10.51. $C_{22}H_{32}Cl_2N_4P_2Ti$ requires C, 49.55; H, 6.05; N, 10.51%. δ_H (C_6D_6) 7.40 (s, 2 H); 7.29 (d, 2 H, J_{HH} = 7.9 Hz), 7.07 (t, 2 H, J_{HH} = 7.7 Hz), 6.72 (d, 2 H, J_{HH} = 7.3 Hz), 2.09 (s, 6 H), 1.16 (s, 18 H, N^{t}Bu); δ_C (C_6D_6) 151.0 (m), 138.9 (s), 128.9 (s), 126.1 (s), 122.5 (m), 118.1 (m), 54.7 (t, J_{PC} = 8.8 Hz), 28.1 (t, J_{PC} = 6.9 Hz); δ_P 127.6 (s).

[{(Bu^{t}NP)$_2$(*p*-TolN)$_2$}TiCl$_2$] (8c). In a manner identical to that used for the synthesis of **8a**, 0.400 mL (2.90 mmol) of triethylamine, 1.50 mL of a titanium tetrachloride stock solution and 0.604 g (1.45 mmol) of **4c** were allowed to react. Dark-red, rod-shaped crystals were recovered for an overall yield of 0.617 g (79.8%). Mp 170–172 °C. Found: C, 49.64; H, 6.31; N, 10.24. $C_{22}H_{32}Cl_2N_4P_2Ti$ requires C, 49.55; H, 6.05; N, 10.51%. δ_H (C_6D_6) 7.39 (d, 4 H, J_{HH} = 8.3 Hz); 6.92 (d, 4 H, J_{HH} = 8.2 Hz), 2.04 (s, 6 H, Me), 1.15 (s, 18 H, N^{t}Bu); δ_C (C_6D_6) 151.5 (s); 134.8 (s), 129.6 (s), 121.4 (d, J_{PC} = 10.5 Hz), 54.7 (t, J_{PC} = 8.6 Hz), 28.1 (t, J_{PC} = 6.8 Hz), 20.7 (s); δ_P (C_6D_6) 128.2 (s).

[{(Bu^{t}NP)$_2$(PhN)$_2$}VCl·THF] (9). At −78 °C a suspension of $VCl_3(THF)_3$ (0.364 g, 0.973 mmol) in toluene was treated with a suspension of **5a** (0.530g, 0.973 mmol) in toluene (10 mL). The reaction mixture was stirred for 12 h while it slowly warmed to RT. The ensuing orange–brown solution was filtered, then concentrated to about half its volume and stored at RT. Yield: 0.382 g (72.2%) of dark-red, octahedral crystals. Mp 163–166 °C. Found: C, 52.70; H, 6.72; N, 10.21. $C_{24}H_{36}ClN_4OP_2V$ requires C, 52.90; H, 6.66; N, 10.28%. $\mu_{eff} = 2.59\mu_B$.

Polymerization studies

Compounds **1**, **2** and **8a** were tested for their activity as polyolefin catalysts in triplicate reactions. The tests were done in a nitrogen-flushed, 250 mL, mechanically-stirred, stainless-steel Parr pressure vessel, equipped with a 200 mL glass liner. In a typical experiment, micromolar amounts of catalyst (30–50 μmol), dissolved in toluene (40 mL), were injected. Then 100 molar equivalents of a standard MAO solution were added by syringe and the vessel was pressurized (1.5×10^6 Pa) with ethylene. The mechanically-stirred reaction mixture was then heated (60 °C) for 1 h. After completion of the reaction, the vessel was vented and examined for the presence of polymer. Compounds **1** and **2** produced no polymer, but **8a** had an activity of 2.0×10^3 g PE (mol catalyst)$^{-1}$ h^{-1} bar^{-1}. Under these conditions Cp_2ZrCl_2 exhibited an activity of 1.2×10^4 g PE (mol catalyst)$^{-1}$ h^{-1} bar^{-1}.

X-Ray crystallography

Compounds 1, 2, 4a, 5a, 6, 8a and 9. All crystals were grown from supersaturated toluene or THF solutions at the indicated temperatures. Suitable, single crystals were coated with oil, affixed to a glass capillary, and centered on the diffractometer in a stream of cold nitrogen. Reflection intensities were collected with a Bruker SMART CCD diffractometer, equipped with an LT-2 low-temperature apparatus, operating at 213 K. Data were measured using ω scans of 0.3° per frame for 30 s until a complete hemisphere had been collected. The first 50 frames were recollected at the end of the data collection to monitor for decay. Cell parameters were retrieved using SMART[25] software and refined with SAINT[26] on all observed reflections. Data were reduced with SAINT, which corrects for Lorentz and polarization factors and decay. An empirical absorption correction was applied with SADABS.[27] The structures were solved by direct methods with the SHELXS-90[28]

program and refined by full-matrix least squares methods on F^2 with SHELXL-97,[29] incorporated in SHELXTL Version 5.10.[30]

Compound 7·$C_6H_5CH_3$. The crystal was sealed inside an argon-filled glass capillary, and the intensity data were collected on a Bruker P4 diffractometer. Three reflections were monitored after every 97 reflections, and the appropriate intensity corrections were applied during data reduction. Reflection data were reduced with XDISK of the SHELXTL-PC program suite, Version 4.1,[30] and the structure was solved by direct-methods with SHELXL-NT, Version 5.10,[31] and refined as described above.

CCDC reference numbers 197168–197175.

See http://www.rsc.org/suppdata/dt/b2/b211009a/ for crystallographic data in CIF or other electronic format.

Acknowledgements

We thank the Chevron Phillips Chemical Company for Research Assistantships to D. F. M. and L. G. and Mr. Ingo Schranz for doing the polymerization tests.

References

1 M. F. Lappert, A. R. Sanger, R. C. Srivastava and P. P. Power, *Metal and Metalloid Amides*, Ellis Horwood, Chichester, 1980; D. J. Cardin, M. F. Lappert and C. L. Raston, *Chemistry of Organo-Zirconium and -Hafnium Compounds*, Halsted Press, New York, 1986; D. E. Wigley, *Prog. Inorg. Chem.*, 1994, **42**, 239; R. R. Schrock, *Acc. Chem. Res.*, 1997, **30**, 9; W. A. Nugent and J. M. Mayer, *Metal-Ligand Multiple Bonds*, Wiley-Interscience, New York, 1988; C. C. Cummins, *Prog. Inorg. Chem.*, 1998, **47**, 685; D. C. Bradley, M. B. Hursthouse, C. W. Newing and A. J. Welch, *J. Chem. Soc., Chem. Commun.*, 1972, 567; C. Airoldi, D. C. Bradley, H. Chudzynska, M. B. Hursthouse, K. M. Abdul Malik and P. R. Raithby, *J. Chem. Soc., Dalton Trans.*, 1980, 2010; R. A. Andersen, *Inorg. Chem.*, 1979, **18**, 1507; R. A. Andersen, *Inorg. Chem.*, 1979, **18**, 1724; R. A. Andersen, D. B. Beach and W. L. Jolly, *Inorg. Chem.*, 1985, **24**, 4741; J. R. Hagadorn and J. Arnold, *Angew. Chem., Int. Ed.*, 1998, **37**, 1729.

2 C. C. Cummins, S. M. Baxter and P. T. Wolczanski, *J. Am. Chem. Soc.*, 1988, **110**, 8731; P. J. Walsh, F. J. Hollander and R. G. Bergman, *J. Am. Chem. Soc.*, 1988, **110**, 8731; C. C. Cummins, C. P. Schaller, G. D. Van Duyne, P. T. Wolczanski, A. W. E. Chan and R. Hoffmann, *J. Am. Chem. Soc.*, 1991, **113**, 2985; J. L. Bennett and P. T. Wolczanski, *J. Am. Chem. Soc.*, 1994, **116**, 2179; C. C. Cummins, G. D. Van Duyne, C. P. Schaller and P. T. Wolczanski, *Organometallics*, 1991, **10**, 164; C. E. Laplaza, A. L. Odom, W. M. Davis, C. C. Cummins and J. D. Protasiewicz, *J. Am. Chem. Soc.*, 1995, **117**, 4999; C. P. Schaller, C. C. Cummins and P. T. Wolczanski, *J. Am. Chem. Soc.*, 1996, **118**, 591.

3 W. A. Herrmann, M. Denk, R. W. Albach, J. Behm and E. Herdtweck, *Chem. Ber.*, 1991, **124**, 683; T. H. Warren, R. R. Schrock and W. M. Davis, *Organometallics*, 1996, **15**, 562; Y. Schrodi, R. R. Schrock and P. J. Bonitatebus, Jr., *Organometallics*, 2001, **20**, 3560; R. R. Schrock, A. L. Casado, J. T. Goodman, L.-C. Liang, P. J. Bonitatebus, Jr. and W. M. Davis, *Organometallics*, 2000, **19**, 5325; C. C. Cummins, R. R. Schrock and W. M. Davis, *Organometallics*, 1992, **11**, 1452; B. Tsuie, D. C. Swenson, R. F. Jordan and J. L. Petersen, *Organometallics*, 1997, **16**, 1392; K. Aoyagi, P. K. Gantzel, K. Kalai and T. D. Tilley, *Organometallics*, 1996, **15**, 923; T. H. Warren, R. R. Schrock and W. M. Davis, *Organometallics*, 1996, **15**, 562.

4 C. H. Winter, P. H. Sheridan, T. S. Lewkebandara, M. J. Heeg and J. W. Proscia, *J. Am. Chem. Soc.*, 1992, **114**, 1095; A. Martin, M. Mena, A. Pérez-Redondo and C. Yélamos, *Organometallics*, 2002, **21**, 3308; H. W. Roesky, Y. Bai and M. Noltemeyer, *Angew. Chem., Int. Ed. Engl.*, 1989, **28**, 754; D. H. Gregory, *J. Chem. Soc., Dalton Trans.*, 1999, 259.

5 D. C. Bradley, M. B. Hursthouse, C. W. Newing and A. J. Welch, *J. Chem. Soc., Chem. Commun.*, 1972, 567; C. Airoldi, D. C. Bradley, H. Chudzynska, M. B. Hursthouse, K. M. Abdul Malik and P. R. Raithby, *J. Chem. Soc., Dalton Trans.*, 1980, 2010; R. A. Andersen, *Inorg. Chem.*, 1979, **18**, 1507; R. A. Andersen, *Inorg. Chem.*, 1979, **18**, 1724.

6 G. D. Whitener, J. R. Hagadorn and J. Arnold, *J. Chem. Soc., Dalton Trans.*, 1999, 1249; J. R. Hagadorn and J. Arnold, *Organometallics*, 1998, **17**, 1355; A. A. Naiini, W. M. P. B. Menge and J. G. Verkade, *Inorg. Chem.*, 1991, **30**, 5009; W. M. P. B. Menge and J. G. Verkade, *Inorg. Chem.*, 1991, **30**, 4628; C. Morton, P. O'Shaughnessy and P. Scott, *Chem. Commun.*, 2000, 2099; P. J. Stewart, A. J. Blake and P. Mountford, *Organometallics*, 1998, **17**, 3271; S. Danièle, P. H. Hitchcock, M. F. Lappert and P. G. Merle, *J. Chem. Soc., Dalton Trans.*, 2002, 13.

7 J. D. Scollard and D. H. McConville, *J. Am. Chem. Soc.*, 1996, **118**, 10008; J. D. Scollard, D. H. McConville and S. J. Rettig, *Organometallics*, 1997, **16**, 1810; J. D. Scollard, D. H. McConville, N. C. Payne and J. J. Vittal, *Macromolecules*, 1996, **29**, 5241.

8 H. J. Chen, R. C. Haltiwanger, T. G. Hill, M. L. Thompson, D. E. Coons and A. D. Norman, *Inorg. Chem.*, 1985, **24**, 4725; I. Schranz, L. Stahl and R. J. Staples, *Inorg. Chem.*, 1998, **37**, 1493; R. R. Holmes and J. A. Forstner, *Inorg. Chem.*, 1963, **2**, 380.

9 L. Grocholl, L. Stahl and R. J. Staples, *J. Chem. Soc., Chem. Commun.*, 1997, 1465.

10 *Ziegler Catalysts*, ed. G. Fink, R. Mülhaupt and H. H. Brintzinger, Springer, Berlin, 1995; *Applied Homogeneous Catalysis with Organometallic Compounds*, ed. B. Cornils and W. A. Herrmann, Verlag Chemie, Weinheim, Germany, 1996.

11 S. Danièle, P. H. Hitchcock, M. F. Lappert and P. G. Merle, *J. Chem. Soc., Dalton Trans.*, 2002, 13.

12 I. Schranz, D. F. Moser, L. Stahl and R. J. Staples, *Inorg. Chem.*, 1999, **38**, 5814.

13 Y. G. Trishin, V. N. Christokletov, A. A. Petrov and V. V. Kosovtsev, *J. Org. Chem. USSR (Engl. Trans.)*, 1975, **11**, 1747.

14 O. J. Scherer and P. Klusmann, *Angew. Chem., Int. Ed. Engl.*, 1969, **8**, 752.

15 H. V. Rasika Dias, W. Jin and Z. Wang, *Inorg. Chem.*, 1996, **35**, 6074.

16 D. F. Moser, C. C. Carrow, L. Stahl and R. J. Staples, *J. Chem. Soc., Dalton Trans.*, 2001, 1246.

17 K. Aoyagi, P. K. Gantzel, K. Kalai and T. D. Tilley, *Organometallics*, 1996, **15**, 923.

18 J. D. Scollard, D. H. McConville, N. C. Payne and J. J. Vittal, *Macromolecules*, 1996, **29**, 5241.

19 R. R. Schrock, A. L. Casado, J. T. Goodman, L.-C. Liang, P. J. Bonitatebus, Jr. and W. M. Davis, *Organometallics*, 2000, **19**, 5325.

20 C. C. Cummins, R. R. Schrock and W. M. Davis, *Organometallics*, 1992, **11**, 1452.

21 C. C. Cummins, J. Lee and R. R. Schrock, *Angew. Chem., Int. Ed. Engl.*, 1992, **31**, 1501.

22 I. Schranz, D. F. Moser, L. Stahl and R. J. Staples, *Inorg. Chem.*, 1999, **38**, 5814.

23 W. Schnick, *Angew. Chem., Int. Ed. Engl.*, 1993, **32**, 806.

24 G. Bai, H. W. Roesky, H.-G. Schmidt and M. Noltemeyer, *Organometallics*, 2001, **20**, 2962; G. Bai, H. W. Roesky, M. Noltemeyer and H.-G. Schmidt, *Organometallics*, 2002, **21**, 2789.

25 SMART V 4.043 Software for the CCD Detector System, Bruker Analytical X-ray Systems, Madison, WI, USA, 1995.

26 SAINT V 4.035 Software for the CCD Detector System, Bruker Analytical X-ray Systems, Madison, WI, USA, 1995.

27 G. M. Sheldrick, SADABS, Program for Area Detector Absorption Correction, Institute for Inorganic Chemistry, University of Göttingen, Germany, 1996. Based on: R. Blessing, *Acta Crystallogr., Sect. A*, 1995, **51**, 33.

28 G. M. Sheldrick, SHELXS-90, Program for Solution of Crystal Structures, University of Göttingen, Germany, 1990.

29 G. M. Sheldrick, SHELXS-97, Program for Solution of Crystal Structures, University of Göttingen, Germany, 1997.

30 SHELXTL 5.10 PC Version, Program Library for Structure Solution and Molecular Graphics, Siemens Analytical X-Ray Instruments, Inc., Madison, WI, USA, 1998.

31 SHELXTL 5.10 NT Version, Program Library for Structure Solution and Molecular Graphics, Bruker Analytical X-ray Systems, Madison, WI, USA, 1999.